Coexistence of cluster configurations in the ^{32}S nucleus

J. Cseh and G. Lévai
Institute of Nuclear Research of the Hungarian Academy of Sciences (ATOMKI), Debrecen, Pf. 51, Hungary-4001

A. Ventura
Centro Dati Nucleari, ENEA, Via Martiri di Monte Sole 4, I-40129 Bologna, Italy
and INFN, Sezione di Bologna, Italy

L. Zuffi
Università di Milano and INFN, Sezione di Milano, V. Celoria 16, I-20133 Milano, Italy
(Received 24 February 1998)

The $T=0$ energy spectrum and the electromagnetic transitions of the ^{32}S nucleus are described in terms of the semimicroscopic algebraic cluster model. $^{28}\mathrm{Si}+\alpha$ and $^{16}\mathrm{O}+^{16}\mathrm{O}$ configurations are considered for the low-lying bands and molecular resonances, respectively. The cluster configurations, including their Hamiltonians, are treated in a unified framework. The densities of high-lying core-plus-alpha-particle states are *predicted* in those energy windows, where good-resolution experiments have been carried out.
[S0556-2813(98)06410-3]

PACS number(s): 21.60.Gx, 21.60.Fw, 21.10.Re

I. INTRODUCTION

Clusterization is known to be important both in the ground-state region and at high excitation energies of light nuclei. The spectrum of cluster states is thus distributed over a very wide energy range. However, due to obvious experimental difficulties, only certain parts of it are usually known. Further complications occur due to the coexistence of different cluster configurations in the same nucleus, such as, for example, alpha-particle states, and molecular resonances of heavy ions. The theoretical understanding of cluster structure involves a multiple task: (i) a unified description of the cluster spectrum is needed, (ii) a consistent treatment of different configurations is required, and (iii) finally, for a truly reliable description, in addition to the reproduction of experimental data, we need to be able to supply some predictions.

For fully microscopic approaches, which combine microscopic model spaces with effective two-nucleon forces, the detailed calculation in the middle of the *sd* shell is very complicated, especially for configurations including shell excitations. On the other hand, fully phenomenologic approaches are easy to apply. These models use phenomenologic cluster-cluster interactions and model spaces that are constructed without taking into account the Pauli principle. They can describe the high-lying part of the spectrum, but usually cannot be applied to the ground-state region, where the effect of the exclusion principle is very important. These treatments contain a considerable amount of ambiguity, partly because of the parameters of their interactions, and more importantly, because of the large uncertainty in the association of model quantum numbers to the experimental states.

Semimicroscopic models, based on microscopic model spaces and phenomenologic interactions, seem to be able to give the best overall description of clusterization. The recently proposed semimicroscopic algebraic cluster model (SACM) [1] has the additional advantage of having an easily solvable formulation of the energy-eigenvalue problem.

As for the structure of the ^{32}S nucleus, microscopic calculations have been carried out only for the ground-state region ([2–4], and references therein). The energy spectrum of the high-lying $^{28}\mathrm{Si}+\alpha$ states [5] and the $^{16}\mathrm{O}+^{16}\mathrm{O}$ molecular resonances [6] were interpreted in terms of different models without direct connection to the microscopic structure or to each other. In this paper we describe the spectra of the three energy regions in a unified way in terms of the SACM. Starting with the analysis of the low-lying spectrum of ^{32}S as $^{28}\mathrm{Si}+\alpha$ configuration (band structure, electromagnetic transitions) and with that of the $^{16}\mathrm{O}+^{16}\mathrm{O}$ resonances, we give a parameter-free prediction for the complete spectrum of the high-lying core-plus-alpha-particle states.

The prediction is based on the concept of multichannel dynamic symmetry, which connects different reaction channels, and consequently, different cluster configurations [7]. This is a composite symmetry in the following sense. On the one hand, it involves dynamically symmetric interactions associated with specific cluster configurations, and having very similar nature, like those of other algebraic models (i.e., having Hamiltonians expressed in terms of invariant operators of an algebra chain). On the other hand, the multichannel symmetry requires an invariance with respect to the transformation of one cluster configuration to another (i.e., from one set of Jacobian coordinates to another). This requirement acts as a strong constraint put on the interactions of different cluster configurations, and as a consequence, it reduces considerably the ambiguity which is present in the phenomenologic description of the spectrum.

In the ground-state region of the ^{32}S nucleus, different shapes seem to coexist. The excitation energies of the low-lying 0^+, 2^+, and 4^+ states suggest a nearly spherical vibrator, while the quadrupole moment of the first 2^+ state [8] corresponds to prolate deformation. Shell model calculations [9] are able to reproduce this shape, as well as the positive parity part of the low-lying spectrum [3,9] in general. Hartree-Fock [10] and Nilsson-Strutinsky [11] calculations give prolate, oblate, and spherical shapes at energies close to

each other, while the SU(3) shell model has a preference for the triaxial shape [12].

In the present work our main goal is to describe the gross features of the large-scale spectrum on a common basis. This includes the treatment of the positive- and negative-parity spectra on the one hand, and the unified description of the different cluster spectra in highly excited regions, on the other. Therefore, our description of the low-lying positive parity spectrum is less detailed than that of the shell model calculations, and it should not be considered as a substitution or competitor. Rather, its main role is to indicate that the model spaces and Hamiltonians we apply for the *unified* treatment of the gross features of the spectrum in a wide energy range are compatible with the fully microscopic description, and are able to account for *some* aspects of the structure in the ground-state region as well.

II. THE SEMIMICROSCOPIC ALGEBRAIC CLUSTER MODEL

This model is algebraic in the sense that both the basis states, and the physical operators are characterized by the irreducible representations of some Lie algebras, and therefore the matrix elements can be determined by group theoretical methods. In the SACM, the internal structure of the clusters is described by the Elliott model of $U_C^{ST}(4)\otimes U_C(3)$ group structure [13], where $U^{ST}(4)$ is Wigner's spin-isospin group [14]. The relative motion is treated in terms of the $U_R(4)$ vibron model [15]. The group structure of the model for a system of two clusters, when one of them has a closed shell structure, is

$$U_C(3)\otimes U_R(4)\supset U_C(3)\otimes U_R(3)\supset SU_C(3)$$

$$\otimes SU_R(3)\supset SU(3)\supset O(3)\supset O(2)$$

$$|[n_1^C,n_2^C,n_3^C],[N,0,0,0],[n_\pi,0,0,],(\lambda_C,\mu_C),$$

$$(n_\pi,0),(\lambda,\mu),\chi,L,M\rangle. \quad (1)$$

Here we have indicated also the labels of irreducible representations (irreps) of the corresponding groups. The superscript and subscript C means ''cluster,'' indicating that the particular group characterizes the internal structure of the non-closed-shell cluster. Similarly, subscript R signifies groups associated with the relative motion of the clusters. The relative motion is characterized by n_π, the number of oscillator quanta (dipole bosons) and N, which sets the higher limit for n_π and thus sets the size of the model space. (λ_C,μ_C) is the $SU_C(3)$ representation associated with the orbital structure of the non-closed-shell (core) nucleus, (λ,μ) is the SU(3) representation assigned to the united nucleus, while the role of χ is to distinguish between O(3) representations which have identical values of L, in case there are several of them belonging to the same SU(3) irreducible representation. It can be interpreted as the projection K of the total angular momentum on a nuclear symmetry axis.

A major point in constructing the model space is related to the exclusion of the Pauli-forbidden states and the spurious excitations of the center-of-mass motion. One can do that by making an intersection between the cluster model basis corresponding to group-chain (1) and that of the (fully antisymmetric) SU(3) shell model of the whole nucleus. This procedure is based on the equivalence of the shell model Hamiltonian and that of the cluster model [16]. The resulting cluster model space is an SU(3) symmetry-dictated truncation of the full shell model space for each cluster configuration. More detailed discussion on the construction of the model space is given in the next section, in relation to the specific configurations we consider here.

The physical operators of the model are expressed in terms of the generators of group chain (1) with parameters to be fitted to the experimental data. An important limit emerges when the Hamiltonian can be expressed in terms of the Casimir invariants of the subgroup chain. This is called dynamic symmetry, and when it holds, an analytic solution of the energy eigenvalue problem is available. Besides the Casimir invariants of the groups appearing in Eq. (1), a Hamiltonian of this kind may contain other terms which are diagonal (or closely diagonal) in the associated basis. These terms may also reflect further types of symmetries, such as those related to the geometric arrangement of the system. A possible Hamiltonian of this type is the following:

$$H=E_0+\gamma_R n_\pi+\delta_R C_2(SU_R(3))+\tau_C C_3(SU_C(3))$$
$$+\delta C_2(SU(3))+(\beta+n_\pi\tilde{\beta})J(J+1)+(\theta+(-1)^{n_\pi}\tilde{\theta})\chi^2$$
$$+\sigma(-1)^{n_\pi+\chi}, \quad (2)$$

where C_n is the nth order Casimir invariant of the SU(3) group, and the subscripts C and R again stand for ''cluster'' and ''relative motion,'' respectively. The physical importance of the individual interaction terms is discussed later on, in Sec. III A 1. We note that although χ^2, which accounts for K-band splitting is not an invariant of the SU(3) group, it is a nearly diagonal higher-order scalar operator constructed from SU(3) generators [17]. In our calculations in the dynamic symmetry approximation, we do not diagonalize it, rather (referring to its small off-diagonal matrix elements) we approximate it with the relevant K^2 value. Our motivation for this is to keep the calculations simple using the dynamical symmetry approximation. In a more sophisticated approach the diagonalization of the Hamiltonian could be performed. We reserve this option for future studies, in which other nondiagonal operators will also be considered in the Hamiltonian.

The operators of the isoscalar electromagnetic transitions can be expressed in terms of the dipole, quadrupole, and angular momentum operators [1]:

$$T^{(E1)}=d_R D_R^{(1)}, \quad (3)$$

$$T^{(E2)}=q_R Q_R^{(2)}+q_C Q_C^{(2)}, \quad (4)$$

$$T^{(M1)}=g_R L_R^{(1)}+g_C L_C^{(2)}. \quad (5)$$

Besides their O(3) tensorial character (i.e., vector of rank-2 tensors) the various dipole and quadrupole operators also carry well-defined $SU_R(3)$ and $SU_C(3)$ tensorial structure, which simplifies the calculation of their matrix elements in the coupled SU(3) basis (1). The parameters appearing in

TABLE I. The SACM model space for the ^{28}Si(0,12)+α, ^{28}Si(12,0)+α, and ^{16}O+^{16}O configurations. The SU(3) states present in the particular channels are displayed for the first few shells.

$n\hbar\omega$	^{28}Si(0,12)+α	^{28}Si(12,0)+α	^{16}O+^{16}O
0	(4,8),(3,7),(2,6),(1,5),(0,4)	(4,8)	—
1	(6,9),(5,8),(4,7),(3,6),(2,5),(1,4),(0,3)	(9,6),(7,7),(5,8),(3,9)	—
2	(8,10),(7,9),(6,8),(5,7),(4,6), (3,5),(2,4),(1,3),(0,2)	(14,4),(12,5),(10,6),(8,7),(6,8), (4,9),(2,10)	—
3	(10,11),(9,10),(8,9),(7,8),(6,7), (5,6),(4,5),(3,4),(2,3),(1,2),(0,1)	(19,2),(17,3),(15,4),(13,5),(11,6), (9,7),(7,8),(5,9),(3,10),(1,11)	—
4	(12,12),(11,11),(10,10),(9,9),(8,8),(7,7), (6,6),(5,5),(4,4),(3,3),(2,2),(1,1),(0,0)	(24,0),(22,1),(20,2),(18,3),(16,4),(14,5), (12,6),(10,7),(8,8),(6,9),(4,10),(2,11),(0,12)	(24,0)

these transition operators are to be fitted to the experimental data, similarly to the parameters of the Hamiltonian (2).

III. CALCULATIONS FOR THE ^{28}Si+α AND ^{16}O+^{16}O CLUSTERIZATIONS

The U(3) irreps into which the states are classified are determined by the distribution of the oscillator quanta along the axes of a Cartesian reference frame $[n_z^C,n_x^C,n_y^C] \equiv [n_1^C,n_2^C,n_3^C]$, according to the prescription of the shell model. The ground-state band of ^{28}Si is considered to belong to the U(3) irrep [16,16,4], and, consequently, to the (0,12) irrep of the SU(3) subgroup. This corresponds to oblate deformation. The ground state of the α-particle and of the ^{16}O nucleus belong to the [0,0,0] and the [4,4,4] U(3) irreps, respectively, and both correspond to the (0,0) SU(3) scalar irrep. We also take into account the ^{28}Si states belonging to the $(\lambda,\mu)=(12,0)$ SU(3) irrep, which corresponds to prolate equilibrium shape. All these clusterizations include states with exclusively $T=0$ isospin.

A unified treatment of the clusterizations is carried out as follows. The cluster model spaces are obtained as those parts of the shell model space that belong to the direct product SU(3) symmetries of the cluster internal structures and the corresponding (Pauli-allowed) relative motions. The model spaces of different clusterizations are obviously different, but they may have considerable overlaps. If the overlapping cluster bands of different configurations have the same energies, we speak of multichannel dynamic symmetry [7]. This means that, e.g., the Hamiltonian of one cluster configuration may completely determine that of another configuration. If this very restrictive symmetry holds, the model has strong predictive power. Let us consider two configurations (denoted by 1 and 2), each containing two clusters characterized by the group-chain (1). If the relation between the relative motion quantum numbers is $n_{\pi 1}=n_{\pi 2}+n_{\pi 0}$, and the integer constant $n_{\pi 0}$ is even (as in our case), then the restrictions of the multichannel dynamic symmetry are the following: $\tau_{C_1}=\tau_{C_2}=0$, $\delta_{R_1}=\delta_{R_2}=\delta_R$, $\gamma_1=\gamma_2+3\delta_r+n_{\pi 0}$, $E_{01}=E_{02}+(\gamma_2+3\delta_R)+n_{\pi 0}$, $\tilde{\beta}_1=\tilde{\beta}_2=\tilde{\beta}$, $\beta_1=\beta_2+\tilde{\beta}n_{\pi 0}$, $\delta_1=\delta_2=\delta$, $\theta_1=\theta_2=\theta$, $\sigma_1=\sigma_2=\sigma$ for the Hamiltonian, and $d_R=d$, $q_R=q_C=q$, $g_C=g_R=g$ for the transition operators. Here the parameters without a channel index indicate channel-independent quantities.

Table I shows the model spaces of the SACM for the ^{28}Si(0,12)+α, ^{28}Si(12,0)+α, and ^{16}O+^{16}O cluster configurations in the first five shells. The cluster states are obtained as triple outer products: $(\lambda_{C_1},\mu_{C_1})\otimes(\lambda_{C_2},\mu_{C_2})\otimes(n_\pi,0)$, where $(\lambda_{C_i},\mu_{C_i})$ stands for the internal structure of cluster i, while $(n_\pi,0)$ are the quantum numbers of the relative motion. Here n_π is limited from below by the Pauli principle: $n_\pi \geqslant 8$ for ^{28}Si+α, and $n_\pi \geqslant 24$ for ^{16}O+^{16}O. However, these product wave functions contain Pauli-forbidden states, too. In order to exclude them we make an intersection with the SU(3) shell model space of the ^{32}S nucleus. This model space is fully antisymmetric. Therefore, the model space that we obtain as an intersection is free from the Pauli-forbidden states. The truncation, as described here, can be carried out due to the equivalence of the SU(3) dynamically symmetric Hamiltonians of the shell and cluster models [16]. One can see from Table I, that for the $0\hbar\omega$ major shell of the ^{32}S nucleus, the Pauli principle rules out several U(3) irreps of the ^{28}Si(12,0)+α configuration, and all irreps of the ^{16}O+^{16}O configuration. With increasing excitation energy, which shows up in the cluster picture as increasing number of oscillator quanta of the relative motion, the number of cluster irreps excluded by the Pauli principle is less and less. But for the low-lying major shells of Table I the truncation is very severe. In particular, the lowest-lying Pauli-allowed ^{16}O+^{16}O cluster configuration belongs to $4\hbar\omega$ excitation of the ^{32}S nucleus.

A particularly interesting question is the relation of the same irreps of different cluster configurations, such as for example (4,8) in the $0\hbar\omega$, and (5,8) in the $1\hbar\omega$ major shell, which appear both in the ^{28}Si(0,12)+α and in the ^{28}Si(12,0)+α configurations, or the (24,0) states being common in the ^{28}Si(12,0)+α and ^{16}O+^{16}O configurations in the $4\hbar\omega$ major shell. These states are not orthogonal to each other; on the contrary, they have very large overlaps. In case the shell model irrep has a single multiplicity, like in these examples, then the fully antisymmetric cluster model wave functions $\psi_{C^{(i)}}=\mathcal{N}_{(i)}\mathcal{A}(\phi_{C_1^{(i)}}\phi_{C_2^{(i)}}\phi_{R^{(i)}})$ of two different configurations may differ from each other only in their normalization factors. Here $\mathcal{N}_{(i)}$ stands for the normalization factor, and $\mathcal{A}$ is the antisymmetrizer operator [18]. In our semimicroscopic treatment we do not derive $\mathcal{N}_{(i)}$ microscopically, rather we simply suppose that the $\psi_{C_k^{(i)}}$'s are normalized to unity. The requirement that these states should have the same energy for different cluster configurations is the basic assumption of the multichannel dynamic symmetry [7]. Obviously, it holds only for very special interactions,

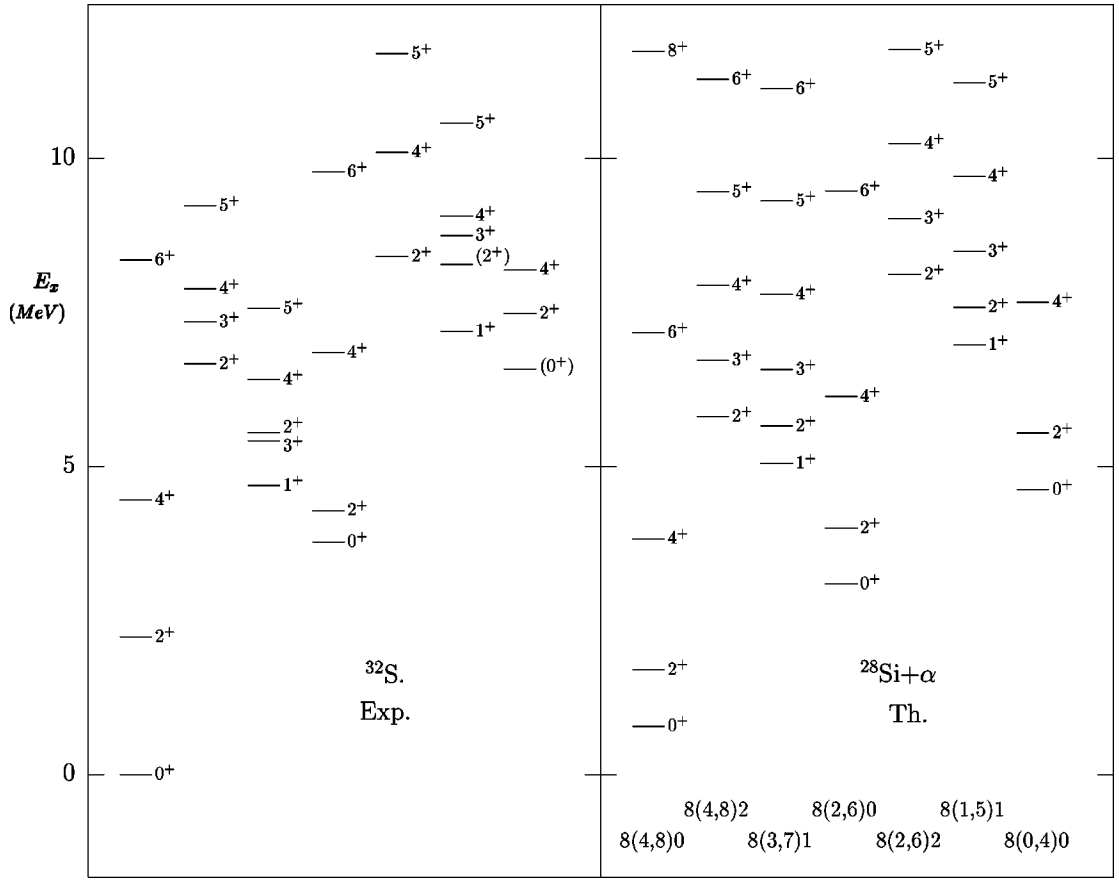

FIG. 1. The low-lying positive-parity states of the ^{32}S nucleus. Experimental states are displayed in the left panel, and the corresponding model spectrum is shown in the right one. The states are arranged into bands that we identified on the basis of their location and their electromagnetic transitions. The J^π assignment of the experimental states is taken from Refs. [2,3]. Uncertain J^π values are given in parentheses. The model spectrum shows the SACM quantum numbers $(\lambda,\mu)\chi$ assigned to the cluster bands, which are supposed to be built on the oblate ^{28}Si ground-state band. All model states belong to the $0\hbar\omega$ shell, which corresponds to $n_\pi=8$.

namely for those ones that are invariant under the transformation from one cluster configuration to the other, i.e., from one set of Jacobi coordinates to the other.

The ^{28}Si$+\alpha$ and ^{16}O$+^{16}$O cluster configurations do not have a common intersection if the Si is in its oblate (0,12) state. But the ^{28}Si(12,0)$+\alpha$ cluster configuration, i.e., prolate core plus alpha-particle states, do have a common intersection with both of them. Therefore, in order to be able to construct channel-invariant interactions, etc., we take into account this configuration as well. It turns out that one can keep a complete symmetry between the ^{28}Si(12,0)$+\alpha$ and ^{16}O$+^{16}$O channels, but a reasonable description of the experimental data requires a slight breaking of the multichannel invariance between the ^{28}Si(0,12)$+\alpha$ and ^{28}Si(12,0) $+\alpha$ configurations. This breaking, however, does not destroy the predictive power of our description, as will be illustrated by our detailed calculations. The strength of the symmetry breaking can be characterized quantitatively.

A. Energy spectrum

In assigning observed $T=0$ ^{32}S levels to the ^{28}Si(0,12) $+\alpha$ cluster model states we have made use of Ref. [2], which extends the existing compilation [8] by adding states with higher J values to it and by clarifying a number of uncertain J^π assignments. This compilation is claimed to be essentially complete for $T=0$ states up to $E_x\simeq 10$ MeV. We also accepted some further J^π assignments made by the same authors based on the analysis of the data in [2] in terms of shell model considerations [3]. In order to establish a band structure of the cluster states we also took into account electromagnetic transition data, such as isoscalar $B(E2)$ [19,20,2], $B(M1)$ [19,20,2], and $B(E1)$ [19,21,20,2] values.

1. Parameters of the Hamiltonian

The low-lying part of the ^{32}S energy spectrum [8] contains bands with both positive and negative parity, and these can be identified with model bands labeled with the $n_\pi(\lambda,\mu)\chi$ quantum numbers of the SACM. The two $K^\pi=0^+$ bands built on the 0_1^+ ground state and the 0_2^+ state at 3.778 MeV can be labeled as 8(4,8)0 and 8(2,6)0. A somewhat staggered $K^\pi=1^+$ band starts at 4.695 MeV, and there is also a 2^+ band at 6.666 MeV. We label these with the quantum numbers 8(3,7)1 and 8(4,8)2. All these states correspond to $0\hbar\omega$ excitations, which means that the relative motion of the core and the α cluster does not carry any excitation quanta in excess of the 8π bosons required by the Pauli principle.

The negative-parity part of the spectrum seems to contain a $K^\pi=3^-$, 1^-, 5^-, and a 0^- band starting at 5.006, 5.798, 6.762, and 7.434 MeV, respectively. We associated the first

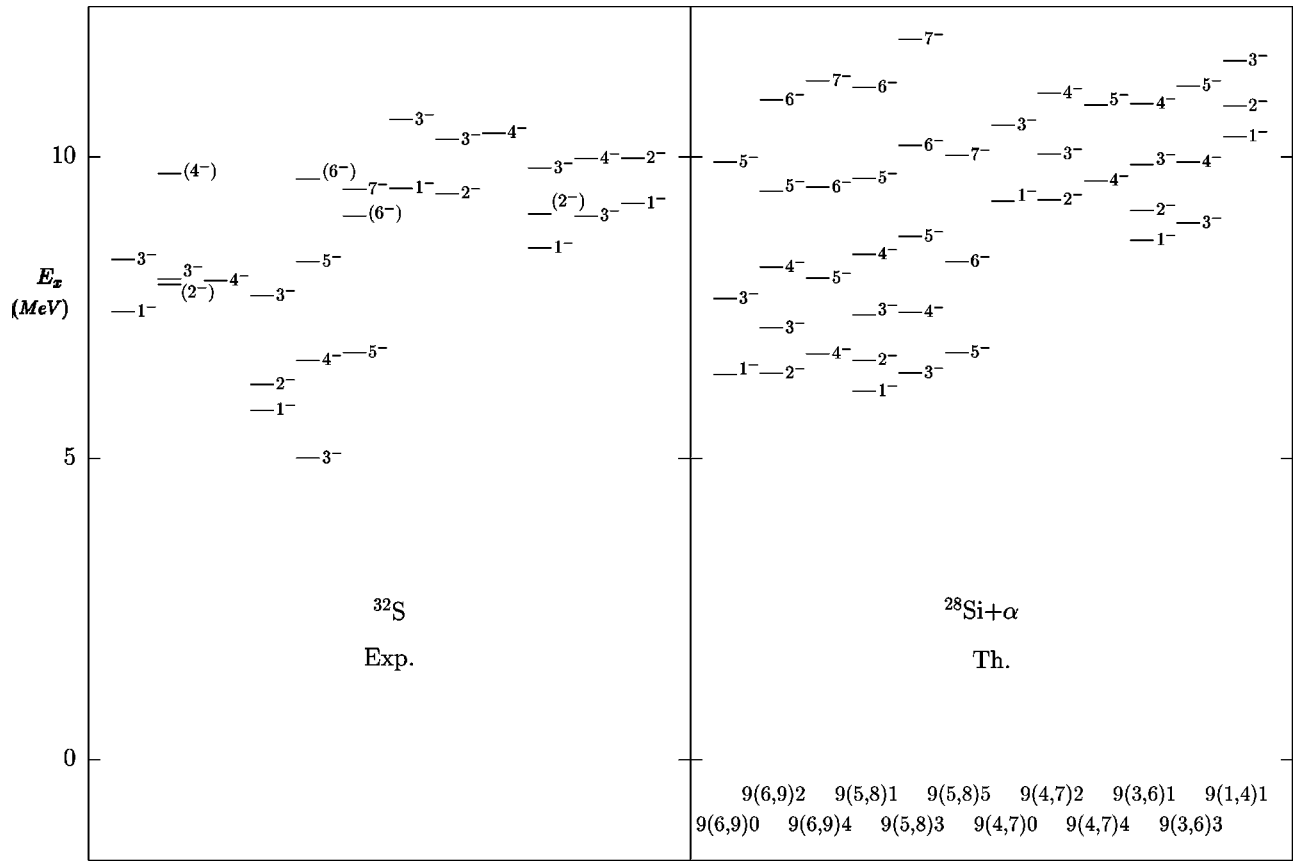

FIG. 2. The same as Fig. 1 for negative parity. The model states are assigned to the $1\hbar\omega$ shell, corresponding to $n_\pi=9$.

three of these to the model bands 9(5,8)3, 9(5,8)1, and 9(5,8)5, and the fourth one to 9(6,9)0.

The $^{16}O+^{16}O$ configuration becomes Pauli allowed in the SACM when there are $n_\pi=24$ π bosons in the relative motion, corresponding to $4\hbar\omega$ excitations of the ^{32}S nucleus. Then the resonances can be assigned to the band 24(24,0)0. The $(\lambda,\mu)=(24,0)$ SU(3) multiplet is missing from the ^{28}Si$(0,12)+\alpha$ model space, however, it is present in the ^{28}Si$(12,0)+\alpha$ one (as a $4\hbar\omega$ excitation), because then it can be obtained from the $(\lambda_C,\mu_C)\times(n_\pi,0)=(12,0)\times(12,0)$ SU(3) outer product.

We used the Hamiltonian of Eq. (2) to fit the ^{32}S spectrum. We fitted the model parameters within a two-step procedure. First we found those parameters that set the relative position of states (bands) within individual major shells ($0\hbar\omega$, $1\hbar\omega$, etc.) and then those that determine the relative position of the shells. According to this, we first set the value of δ, mainly based on positive-parity bands in the ground-state region, and fitted β, $\tilde{\beta}$, θ, and $\tilde{\theta}$. The first two of these set the rotational constant of bands from the various shells, imitating the observed feature that bands with higher excitations of the relative motion seem to have higher moment of inertia. The second pair accounts for (a parity-dependent) K-band splitting within SU(3) multiplets. The parity dependence seems to be an important feature here, because bands with larger K (χ in the SACM) are located higher in the positive-parity spectrum, while they tend to be lower in the negative-parity part.

The parameters obtained (in units of MeV) in the multistep fitting procedure of the Hamiltonian are $E_0=-50.3040$, $\delta_R=-0.292\,60$, $\tau_C=0.002\,291$, $\delta=-0.032\,00$, $\beta=0.360\,93$, $\tilde{\beta}=-0.0261$, $\theta=0.453\,70$, $\tilde{\theta}=0.574\,24$, and $\sigma=-0.842\,99$. τ_C and the corresponding interaction term accounts for the splitting between ^{28}Si$+\alpha$ states built on oblate and prolate core states, and it does not respect the multichannel dynamic symmetry. γ_R, the coefficient of the harmonic oscillator term was not fitted, rather it was set to 11.6939 MeV, the oscillator constant considered usually for $A=32$ nuclei: $\gamma_R=45A^{-1/3}-25A^{-2/3}$.

The last term of the Hamiltonian (2) has not been considered in our model previously, therefore we discuss it here in some detail. The introduction of this phenomenologic term seems to be essential to describe the observed spectral patterns of the ^{32}S nucleus, which indicate that bands with even K are usually located higher in positive-parity shells and lower in negative-parity shells, while the situation is reversed for bands with odd K. This term, for example, prevents bands with K high and even from appearing too low in the negative-parity part of the spectrum. The interpretation of this term can be given in terms of several frameworks.

First, it is related to the parity of the states (determined by the number of excitation quanta carried by the system) and also to the parity (i.e., the even or odd nature) of χ, the projection of the angular momentum on a symmetry axis. Both of these are well-defined quantities in the shell model framework. Since the parity of χ is related to that of the smaller of the quantum numbers λ and μ in the SU(3) scheme, $(-1)^{n_\pi+\chi}$ can be expressed in terms of $(-1)^{n_i}$, where n_i is the number of oscillator quanta associated with the three spatial directions in the Cartesian frame. Usually

the $n_z \geq n_x \geq n_y$ convention is used to label the principal axes. It can be shown then that for cluster systems consisting of even-even clusters without major shell excitations $(-1)^{n_\pi+\chi}$ is equal with $(-1)^{n_z}$ if $\lambda \geq \mu$ holds, and with $(-1)^{n_y}$ otherwise. (We recall the definition $\lambda = n_z - n_x$ and $\mu = n_x - n_y$.)

This interpretation can be linked with an additional symmetry of the system, the D_2 point symmetry of a general triaxial object associated with the rotations through π about its principal axes [22]. It is known [23] that the SU(3) irreps associated with the states of a general triaxial nucleus, such as ^{32}S, can be classified according to their transformation properties with respect to the elements of the D_2 symmetry group. In particular, these states can be divided according to the four one-dimensional irreps of D_2, labeled by the factors ± 1 associated with the rotations by π through two perpendicular symmetry axes. In the SU(3) framework these phase factors are supplied by $(-1)^\lambda$ and $(-1)^\mu$ [23]. Straightforward calculation shows that for all the $^{28}\mathrm{Si}(0,12)+\alpha$ states listed in Table I and plotted in Figs. 1 and 2, $(-1)^{n_\pi+\chi}$ is equal to $(-1)^\mu$. This seems to indicate that the phenomenologic last term of Eq. (2), which depends on quantities associated with the geometric content of our essentially algebraic approach (i.e., n_π and χ), indeed, reflects the spatial arrangement of the nuclear system.

In order to characterize the breaking of the multichannel symmetry in a quantitative way, we calculate the parameter $b = \tau_C^2/(\tau_C^2 + \Sigma_i \alpha_i^2)$, where τ_C is the strength of the term which does not respect the multichannel symmetry, and α_i's stand for the strengths of the symmetry-preserving terms of the Hamiltonian. The parameters of our Hamiltonian (2) correspond to a 4×10^{-8} breaking of the multichannel symmetry. We note here that this seemingly small breaking is due to the small value of τ_C. The actual magnitude of the symmetry-breaking term $\tau_C C_3(\mathrm{SU}_C(3))$ in the Hamiltonian is 11.134 MeV, with negative and positive sign for states built on the oblate and the prolate ^{28}Si configurations, respectively.

Altogether we considered 28 states from both the $0\hbar\omega$ and the $1\hbar\omega$ shell, and 24 states (corresponding to ^{16}O $+ ^{16}$O resonances) from the $4\hbar\omega$ shell. We assigned the states into bands according to their location and electromagnetic transitions (see below). The resulting spectrum is displayed in Figs. 1, 2, and 3 for the low-lying positive- and negative-parity states, and the $^{16}\mathrm{O}+^{16}\mathrm{O}$ resonances.

In the low-lying spectrum the model essentially exhausts the experimental data set for the level scheme of the ^{32}S nucleus up to $E_x \simeq 8$ to 10 MeV, depending on J^π. In particular, the first unaccounted experimental 0^+ state is located at 7.637 MeV; for 1^+ this happens at 9.290 MeV, for 2^+ at 8.690 MeV, and for 3^+ at 9.920 MeV. The corresponding values for the negative-parity states are 9.731, 8.380, and 10.434 MeV, for the 1^-, 2^-, and 3^- states, respectively. We note that the cluster model space does not contain any 0^- state, of which the lowest one is located at 10.402 MeV. (In the assignment of the excitation energies we accepted the results of Ref. [2].) The $0\hbar\omega$ model space contains altogether three $J^\pi = 0^+$ states. The third one of these with $(\lambda,\mu) = (0,4)$ SU(3) labels appears near 5 MeV in the model spectrum. We assigned this state to the experimental level at

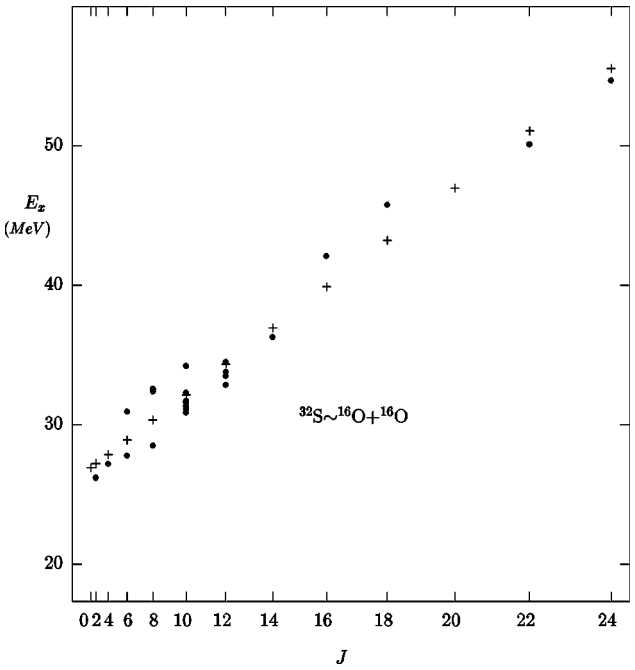

FIG. 3. The $^{16}\mathrm{O}+^{16}\mathrm{O}$ molecular resonances displayed in a rotational diagram form. Data on the experimental states (●) are from Ref. [6]. The model states (+) belong to the $4\hbar\omega$ shell, which corresponds to $n_\pi = 24$ for the $^{16}\mathrm{O}+^{16}\mathrm{O}$ configuration and to $n_\pi = 12$ for the $^{28}\mathrm{Si}+\alpha$ clusterization based on the excited prolate ^{28}Si band.

$E_x = 6.581$ MeV, which is known to have $J = 0-4$ and natural parity [2]. The interpretation of this state is not equivocal: it has been assigned previously to $J^\pi = 0^+$ [24] and 4^+ [3] alike.

Since the model space constructed assuming inert ^{16}O clusters contains only one state for any given J value (up to $J = 24$) we fitted the average position of the experimental states for each angular momentum. We also note that in the $^{16}\mathrm{O}+^{16}\mathrm{O}$ channel, only states with $J = even$ were identified experimentally, due to the identical nature of the clusters. We, therefore, displayed only these states in the model spectrum. A richer spectrum of $^{16}\mathrm{O}+^{16}\mathrm{O}$ resonances could be generated in the $4\hbar\omega$ model space if we had permitted exci-

TABLE II. The number of states predicted by the U(3) symmetry in comparison with the number of resonances reported in Ref. [25].

	Energy windows		Number of states	
J^π	E_x(min)	E_x(max)	Model	Exp.
0^+	10.37	11.13	1	6
2^+	10.87	11.96	4	3
3^-	10.82	12.20	4	8
3^-	12.94	14.43	6	10
4^+	13.69	15.85	11	7
5^-	13.87	17.26	22	15
6^+	15.75	17.87	19	9
7^-	17.39	20.28	22	13
8^+	18.80	20.45	11	13
9^-	21.21	23.30	16	10

TABLE III. Reduced $E2$ transition probabilities (in W.u.) between ^{32}S states. Experimental data are from Refs. [21,19,2].

Experimental data			Theory		
$J_i^\pi(E_{x\,i})$	$J_f^\pi(E_{x\,f})$	$B(E2)_{\text{Expt.}}$	$B(E2)_{\text{Th.}}$	$n_\pi(\lambda,\mu)\chi\ i\to f$	
$2^+(2.230)$	$0^+(0.0)$	10 ± 1	7.27	8(4,8)0	8(4,8)0
$4^+(4.459)$	$2^+(2.230)$	12 ± 2	9.17		8(4,8)0
$6^+(8.346)$	$4^+(4.459)$	>3.7	7.88		8(4,8)0
$2^+(6.666)$	$0^+(0.0)$		1.06	8(4,8)2	8(4,8)0
	$2^+(2.230)$		1.11		8(4,8)0
	$4^+(4.459)$		0.005		8(4,8)0
	$1^+(4.695)$		1.25		8(3,7)1
	$3^+(5.413)$		1.34		8(3,7)1
$4^+(7.883)$	$2^+(2.230)$		0.77		8(4,8)0
	$2^+(5.549)$		2.86		8(3,7)1
$5^+(9.235)$	$4^+(4.459)$		1.88		8(4,8)0
	$3^+(5.413)$		3.87		8(3,7)1
$1^+(4.695)$	$2^+(2.230)$		5.58	8(3,7)1	8(4,8)0
$2^+(5.549)$	$0^+(0.0)$	0.12 ± 0.03	1.44		8(4,8)0
	$2^+(2.230)$		0.68		8(4,8)0
	$1^+(4.695)$		7.32		8(3,7)1
$3^+(5.413)$	$2^+(2.230)$	2.7 ± 0.5	0.89		8(4,8)0
	$4^+(4.459)$		4.27		8(4,8)0
	$1^+(4.695)$		7.50		8(3,7)1
	$2^+(5.549)$		8.75		8(3,7)1
$4^+(6.411)$	$2^+(2.230)$	3.0 ± 0.7	1.15		8(4,8)0
	$2^+(5.549)$		6.68		8(3,7)1
	$3^+(5.413)$		0.96		8(3,7)1
$5^+(7.567)$	$4^+(4.459)$	2.1 ± 0.5	0.71		8(4,8)0
	$3^+(5.413)$		9.30		8(3,7)1
$0^+(3.778)$	$2^+(2.230)$	14 ± 2	0	8(2,6)0	8(4,8)0
	$2^+(5.549)$		15.91		8(3,7)1
$2^+(4.282)$	$0^+(0.0)$	1.4 ± 0.2	0		8(4,8)0
	$2^+(2.230)$	9.3 ± 1.3	0		8(4,8)0
	$1^+(4.695)$		2.89		8(3,7)1
	$2^+(5.549)$		0.71		8(3,7)1
	$0^+(3.778)$		8.13		8(2,6)0
$4^+(6.852)$	$4^+(4.459)$	$0.9^{+0.7}_{-0.5}$	0		8(4,8)0
	$2^+(4.282)$	$5.9^{+3.1}_{-1.4}$	9.50		8(2,6)0
	$2^+(5.549)$		0.74		8(3,7)1
	$3^+(5.413)$		1.80		8(3,7)1
	$4^+(6.411)$		0.10		8(3,7)1
$6^+(9.783)$	$4^+(4.459)$	$0.23^{+0.8}_{-0.1}$	0		8(4,8)0
	$4^+(6.852)$		6.58		8(2,6)0
$2^+(8.407)$	$1^+(4.695)$		0.60	8(2,6)2	8(3,7)1
	$3^+(5.413)$		1.60		8(3,7)1
	$0^+(3.778)$		0.84		8(2,6)0
	$2^+(4.282)$		0.80		8(2,6)0
$4^+(10.102)$	$2^+(4.282)$		0.60		8(2,6)0
$2^+(8.281)$	$2^+(4.282)$		0.67	8(1,5)1	8(2,6)0
$3^+(8.746)$	$2^+(4.282)$		0.76		8(2,6)0
$4^+(9.065)$	$2^+(4.282)$		0.81		8(2,6)0
$5^+(10.574)$	$4^+(8.191)$		4.24		8(0,4)0
$2^+(9.464)$	$0^+(0.0)$	0.8 ± 0.3		$n_\pi=10$	8(4,8)0
$2^+(9.712)$	$0^+(0.0)$	0.026 ± 0.009		$n_\pi=10$	8(4,8)0
$3^+(10.221)$	$2^+(2.230)$	0.01 ± 0.005		$n_\pi=10$	8(4,8)0
	$1^+(4.695)$	1.6 ± 0.4		$n_\pi=10$	8(3,7)1
$1^+(10.232)$	$3^+(5.413)$	1.3 ± 0.7		$n_\pi=10$	8(3,7)1

TABLE III. (*Continued.*)

Experimental data			Theory		
$J_i^\pi(E_{xi})$	$J_f^\pi(E_{xf})$	$B(E2)_{\text{Expt.}}$	$B(E2)_{\text{Th.}}$	$n_\pi(\lambda,\mu)\chi i\rightarrow f$	
$4^-(7.950)$	$3^-(5.006)$	2.8 ± 0.7	3.38	9(6,9)4	9(5,8)3
$4^-(6.621)$	$3^-(5.006)$	10 ± 2	11.36	9(5,8)3	9(5,8)3
$5^-(8.270)$	$3^-(5.006)$	>5.9	2.65		9(5,8)3
$6^-(9.635)$	$4^-(6.621)$	5.9^{+12}_{-2}	4.23		9(5,8)3
$6^-(9.024)$	$4^-(6.621)$	1.9 ± 0.5	1.06	9(5,8)5	9(5,8)3
	$5^-(6.762)$	5.6 ± 1.3	10.23		9(5,8)3
$7^-(9.463)$	$5^-(6.762)$	>13	1.72		9(5,8)5
$1^-(9.487)$	$3^-(5.006)$	1.4 ± 0.5	0.02	9(4,7)0	9(5,8)3
$4^-(10.398)$	$3^-(5.006)$	0.1 ± 0.06	0.90	9(4,7)4	9(5,8)3
	$4^-(6.621)$	0.5 ± 0.4	1.05		9(5,8)3

tations of one of the ^{16}O clusters and had broken the SU(3) dynamic symmetry, allowing thus the mixing of various SU(3) representations.

2. Spectrum generation

Having determined the parameters of the Hamiltonian from the ground-state and $^{16}O+^{16}O$ molecular resonance region, we can predict the number of α-cluster states at the intermediate energies. This is just where the elastic alpha-scattering experiments can reveal the resonant states. We have applied the Hamiltonian in Eq. (2), and calculated the number of $^{28}Si(0,12)+\alpha$ states with specific angular momentum in energy windows, where they have been observed. The model space we considered extended to $8\hbar\omega$ excitations. The result is given in Table II in comparison with the data of Ref. [25].

Considering the high excitation energies and the exponential energy dependence of the state densities, the result seems to be quite remarkable. The point to be stressed here is that a comparison with the experimental data on this basis is completely free from any ambiguity, and these densities are obtained without fitting any parameter in this region, or without any model assumption related to the data in question.

B. Electromagnetic transitions

We have considered experimental information on the $B(E2)$, $B(M1)$, and $B(E1)$ values from Refs. [19,21,20,2]. Some of these represent only an upper or lower limit for the given reduced electromagnetic transition rate. The present version of the SACM can describe only isoscalar $E2$, $M1$, and $E1$ transitions. This did not pose a serious problem for the electric quadrupole and dipole transitions. In the case of the magnetic dipole transitions, however, the significant $T=1$ component of a number of states resulted in enhanced $B(M1)$ values due to the dominantly isovector $M1$ transitions [3]. Due to this fact and also to the low number of data, we restricted our study to isoscalar electric quadrupole and dipole transitions only.

The available experimental information on $B(E2)$ values of isoscalar electric quadrupole transitions is limited to about 20 data in the positive-parity domain of the spectrum and about 10 in the negative-parity one. (See Table III for the

TABLE IV. Reduced $E1$ transition probabilities (in 10^{-3} W.u.) between ^{32}S states. The experimental data are from Refs. [19–21,2].

Experimental data			Theory		
$J_i^\pi(E_{x\,i})$	$J_f^\pi(E_{x\,f})$	$B(E1)_{\text{Expt.}}$	$B(E1)_{\text{Th.}}$	$n_\pi(\lambda,\mu)\chi\ \ i\rightarrow f$	
$1^-(5.789)$	$0^+(0.0)$	0.5 ± 0.2	0.242	9(5,8)1	8(4,8)0
	$2^+(2.230)$		0.102		8(4,8)0
$2^-(6.224)$	$2^+(2.230)$	0.18 ± 0.03	0.333		8(4,8)0
$3^-(7.702)$	$2^+(2.230)$		0.237		8(4,8)0
	$4^+(4.459)$		0.118		8(4,8)0
$3^-(5.006)$	$2^+(2.230)$	0.079 ± 0.014	0.000	9(5,8)3	8(4,8)0
$4^-(6.621)$	$4^+(4.459)$	0.032 ± 0.007	0.000		8(4,8)0
	$3^+(5.413)$	0.012 ± 0.002	0		8(3,7)1
$1^-(9.487)$	$0^+(0.0)$	0.54 ± 0.14	0.085	9(4,7)0	8(4,8)0
	$2^+(2.230)$		0.223		8(4,8)0
	$0^+(4.282)$	0.31 ± 0.08	0		8(2,6)0
$3^-(10.626)$	$2^+(2.230)$		0.086		8(4,8)0
	$4^+(4.459)$		0.221		8(4,8)0

details.) We used the electric quadrupole operator of Eq. (4) to describe these transitions. The SU(3) selection rules for this operator are $\Delta\lambda=\Delta\mu=0$ or ±1. We determined the two parameters from a least-square fit to all the available allowed transitions, and we obtained $q_R=0.88\,41\ e\ \mathrm{fm}^2$ and $q_C=-1.93\,83\ e\ \mathrm{fm}^2$. (In the fitting procedure we used the inverse of the relative error as the weight for each transition.) The results are displayed in Table III. In-band transitions are reasonably reproduced, but the strength of the interband ones is sometimes underestimated. Also, the above $T^{(E2)}$ operator forbids transitions from the $K^\pi=0_2^+$ band to the ground-state one, since these transitions correspond to changing the SU(3) quantum numbers λ and μ by two units. These findings can be considered as indications for the breaking of the SU(3) dynamic symmetry: a mixing between the 2^+ states of the $(\lambda,\mu)=(4,8)$, (3,7), and (2,6) SU(3) multiplets would allow relatively strong $B(E2)$ values here, as can be seen in Table III.

In Table III we displayed a number of transitions where no experimental data are available, nevertheless, some estimations are given for them in the literature. Generally, the expectations based on shell model calculations [3] are in reasonable agreement with our results. We also displayed data on some positive-parity levels around $E_x\simeq10$ MeV, which we did not assign to model states. In the SACM these might be interpreted as states with $2\hbar\omega$ excitation. The lowest-lying states from this shell are expected to appear in this energy region, and the (λ,μ) quantum numbers associated with them might be (8,10) or (7,9), etc. (See Tables I and III.) Transitions from these states to the lowest-lying positive-parity states can be calculated using a higher-order term in the $E2$ transition operator, which acts only on the relative motion part of the coupled wave function and changes n_π with 2 units [26–28]. This operator can also change λ and μ up to 2 units, so the $2\hbar\omega\rightarrow0\hbar\omega$ transitions mentioned above are expected to be highly forbidden in the SACM due to the large differences in λ and μ. This is in agreement with the observations: the $B(E2)$ values for these transitions were found to be rather small experimentally.

It is remarkable that although the spectrum of the negative-parity states is not reproduced too well by the model, the calculated $E2$ transition rates seem to support the band assignment of these states, because the $B(E2)$ values are reproduced reasonably well. A similar situation was found in the application of the SACM to other nuclei in the sd shell, such as ^{24}Mg [27] and ^{38}Ar [28].

We note that the more restrictive version of the $T^{(E2)}$ operator with $q_R=q_C\equiv q$ allows transitions exclusively within the same SU(3) irreducible representations, i.e., with $\Delta\lambda=\Delta\mu=0$ only. Using this operator in the fitting procedure we obtained $q=-1.8113\ e\ \mathrm{fm}^2$ and found that the $B(E2)$ values of the intraband transitions changed by up to 10%, while the interband transitions (at least those changing λ and μ) became forbidden. We note that if we assume that the multichannel dynamic symmetry holds between the $^{28}\mathrm{Si}+\alpha$ and the $^{16}\mathrm{O}+^{16}\mathrm{O}$ channels, then we can use this q parameter to make predictions for the strength of $E2$ transitions between the $^{16}\mathrm{O}+^{16}\mathrm{O}$ resonances. With these assumptions we found these to range between 15 to 40 W.u.

A possible consistency check is to analyze $E2$ transitions and quadrupole momenta of the core nucleus, ^{28}Si. Using the parameter q_C determined from the least-square fit of the $B(E2)$ values of transitions between ^{32}S states, we obtain the following data for ^{28}Si: $B(E2;2_1^+\rightarrow0_1^+)=13.39$ W.u., $B(E2;4_1^+\rightarrow2_1^+)=18.05$ W.u., and $B(E2;6_1^+\rightarrow4_1^+)=17.79$ W.u. These are in reasonable agreement with the experimental values of 13 ± 1, 13 ± 1, and 10 ± 3 W.u., respectively. The calculated electric quadrupole moment of the 2_1^+ ^{28}Si state, $Q=16.76\ e\ \mathrm{fm}^2$ also compares favorably with the experimental value $16.5\pm1.8\ e\ \mathrm{fm}^2$.

The situation is somewhat different for ^{32}S: Calculating the electric quadrupole moment of the first excited state we find $Q(2_1^+)=14.39\ e\ \mathrm{fm}^2$, while the experimental value is $-14.9\ e\ \mathrm{fm}^2$. This shows that the SACM reproduces correctly the magnitude of this quadrupole moment, but it predicts oblate, rather than prolate shape for it. In fact, the $(\lambda,\mu)=(4,8)$ SU(3) labels suggest triaxial shape. This finding can again be an indication for the necessity of symmetry breaking: a mixture from the $(\lambda,\mu)\chi=(4,8)2$, $J^\pi=2^+$ state or from $^{28}\mathrm{Si}(12,0)+\alpha$-type states in the $2\hbar\omega$ shell could shift the quadrupole moment to the prolate direction.

The available information on isoscalar $E1$ transitions in ^{32}S is listed in Table IV, along with the theoretical values. The electric dipole operator of the SACM [Eq. (3)] acts only on the relative motion part of the cluster wave function. The selection rules for this operator are $\Delta n_\pi=\pm1$; $\Delta\lambda=\pm1$, $\Delta\mu=0$ or $\Delta\lambda=0$, $\Delta\mu=\mp1$.

The least-square fit procedure of the $B(E1)$ data gave $d_R=0.002\,726\ (\mathrm{W.u.})^{1/2}$. It can be seen from Table IV that the calculated values are in reasonable agreement with the experimental ones. Electric dipole transitions predicted to be forbidden or very weak by the model usually have weak experimental $B(E1)$ values (lying in the $\simeq10^{-5}$ W.u. range).

IV. SUMMARY AND CONCLUSIONS

In this paper we have presented the results of our calculations within the framework of the semimicroscopic algebraic cluster model for the cluster structure of the ^{32}S nucleus. The $^{28}\mathrm{Si}+\alpha$ and $^{16}\mathrm{O}+^{16}\mathrm{O}$ configurations were taken into account. A unified treatment and a single Hamiltonian were used for the energy spectrum of the ground-state region and the $^{16}\mathrm{O}+^{16}\mathrm{O}$ molecular resonances. Based on this Hamiltonian, a parameter-free prediction could be made for the densities of $^{28}\mathrm{Si}+\alpha$ states in the resonance region. It compares reasonably well with the experimental findings. Electric dipole and quadrupole transitions have also been calculated.

The results illustrate that the algebraic model is able to describe a large amount of experimental data in a consistent way. The predictive power of the model for the densities of high-lying cluster states is especially remarkable.

ACKNOWLEDGMENTS

The authors are indebted to Professor M. Brenner for providing them with experimental data, and to Dr. K. W. Burn for a critical reading of the manuscript. This work was supported by the OTKA (Grant No. T22187), INFN, and ENEA.

[1] J. Cseh, Phys. Lett. B **281**, 173 (1992); J. Cseh and G. Lévai, Ann. Phys. (N.Y.) **230**, 165 (1994).
[2] J. Brenneisen, B. Erhardt, F. Glatz, Th. Kern, R. Ott, H. Röpke, J. Schmelzlin, P. Siedle, and B. H. Wildenthal, Z. Phys. A **357**, 157 (1997).
[3] J. Brenneisen, B. Erhardt, F. Glatz, Th. Kern, R. Ott, H. Röpke, J. Schmelzlin, P. Siedle, and B. H. Wildenthal, Z. Phys. A **357**, 377 (1997).
[4] A. Kangasmäki, P. Tikkanen, J. Keinonen, W. E. Ormand, S. Raman, Zs. Fülöp, Á. Z. Kiss, and E. Somorjai, Phys. Rev. C **58**, 699 (1998).
[5] A. Ludu, A. Sandulescu, W. Greiner, K. M. Källman, M. Brenner, T. Lönnroth, and P. Manngard, J. Phys. G **21**, L41 (1995).
[6] U. Abbondanno, Trieste Report No. INFN/Be-91/1991.
[7] J. Cseh, Phys. Rev. C **50**, 2240 (1994).
[8] P. M. Endt, Nucl. Phys. **A510**, 1 (1990).
[9] B. H. Wildenthal, in *Progress in Particle and Nuclear Physics*, edited by D. H. Wilkinson (Pergamon, Oxford, 1984), Vol. 11, p. 5.
[10] I. Morrison, Phys. Lett. **91B**, 4 (1980).
[11] R. K. Sheline, P. C. Sood, and I. Ragnarsson, in *Capture Gamma-ray Spectroscopy*, Pacific Grove, CA 1990, edited by R. Hoff, AIP Conf. Proc. No. 238 (AIP, New York, 1991), p. 533.
[12] M. Harvey, Adv. Nucl. Phys. **1**, 67 (1968).
[13] J. P. Elliott, Proc. R. Soc. London, Ser. A **245**, 128 (1958); **245**, 562 (1958).
[14] E. P. Wigner, Phys. Rev. **51**, 106 (1937).
[15] F. Iachello and R. D. Levine, J. Chem. Phys. **77**, 3046 (1982); F. Iachello, J. Cseh, and G. Lévai, Heavy Ion Phys. **1**, 91 (1995).
[16] K. Wildermuth and Th. Kanellopoulos, Nucl. Phys. **7**, 150 (1958); J. Cseh, G. Lévai, P. O. Hess, K. F. Pál, K. Varga, and W. Scheid, in *Proceedings of the XXI International Colloquium on Group Theoretical Methods in Physics*, Goslar, Germany, 1996, edited by H. D. Doebner, W. Scherer, and C. Schulte (World Scientific, Singapore, 1997), Vol. II, p. 800.
[17] H. A. Naqvi and J. P. Draayer, Nucl. Phys. **A516**, 351 (1990).
[18] K. Wildermuth and Y. C. Tang, *A Unified Theory of the Nucleus* (Academic, New York, 1977).
[19] J. Vernotte *et al.*, Nucl. Phys. **A212**, 493 (1973).
[20] P. M. Endt, At. Data Nucl. Data Tables **55**, 171 (1993).
[21] P. M. Endt, At. Data Nucl. Data Tables **23**, 3 (1979).
[22] A. Bohr and B. R. Mottelson, *Nuclear Structure Vol. II* (W. A. Benjamin, Reading, MA, 1975), p. 179.
[23] D. J. Rowe, M. G. Vassanji, and J. Carvalho, Nucl. Phys. **A504**, 76 (1989).
[24] G. M. Crawley, C. Djalali, N. Marty, M. Morlet, A. Willis, N. Anantaraman, B. A. Brown, and A. Galonsky, Phys. Rev. C **39**, 311 (1989).
[25] A. E. Antropov *et al.*, in *Proceedings of the 7th International Conference on Nuclear Reaction Mechanism*, Varenna, Italy, 1994, edited by E. Gadioli (Università degli Studi di Milano, Milano, 1994), p. 430; K.-M. Källman, Z. Phys. A **356**, 287 (1996).
[26] G. Lévai, J. Cseh, and W. Scheid, Phys. Rev. C **46**, 548 (1992).
[27] J. Cseh, G. Lévai, and W. Scheid, Phys. Rev. C **48**, 1724 (1993).
[28] Zs. Fülöp, G. Lévai, E. Somorjai, Á. Z. Kiss, J. Cseh, P. Tikkanen, and J. Keinonen, Nucl. Phys. **A604**, 286 (1996).